RESEARCH ARTICLE

NUPR1 protects liver from lipotoxic injury by improving the endoplasmic reticulum stress response

Maria Teresa Borrello[1] [ID] | **Maria Rita Emma[2]** | **Angela Listi[1]** | **Marion Rubis[1]** | **Sergiu Coslet[3]** | **Giuseppa Augello[2]** | **Antonella Cusimano[2]** | **Daniela Cabibi[4]** | **Rossana Porcasi[4]** | **Lydia Giannitrapani[4]** | **Maurizio Soresi[4]** | **Gianni Pantuso[5]** | **Karen Blyth[6]** | **Giuseppe Montalto[4]** | **Christopher Pin[7]** | **Melchiorre Cervello[2]** | **Juan Iovanna[1]**

[1]Centre de Recherche en Cancérologie de Marseille, INSERM U1068, CNRS UMR 7258, Aix-Marseille Université and Institut Paoli-Calmettes, Parc Scientifique et Technologique de Luminy, Marseille, France

[2]Istituto per la Ricerca e l'Innovazione Biomedicale (IRIB), Consiglio Nazionale Delle Ricerche, Palermo, Italy

[3]MI-mAbs, Aix-Marseille University, Parc Scientifique et Technologique de Luminy, Marseille, France

[4]Dipartimento di Promozione della Salute, Materno-Infantile, Medicina Interna e Specialistica di Eccellenza (PROMISE), University of Palermo, Palermo, Italy

[5]Department of Surgical Oncological and Oral Sciences, Division of General and Oncological Surgery, University of Palermo, Palermo, Italy

[6]Cancer Research UK Beatson Institute, Glasgow, UK

[7]Children's Health Research Institute, The University of Western Ontario, London, ON, Canada

Correspondence
Melchiorre Cervello, Istituto per la Ricerca e l'Innovazione Biomedica (IRIB), Consiglio Nazionale delle Ricerche (CNR), Via Ugo La Malfa n. 153, 90144 Palermo, Italy.
Email: melchiorre.cervello@irib.cnr.it

Juan Iovanna, Centre de Recherche en Cancérologie de Marseille (CRCM), INSERM U1068, CNRS UMR 7258, Aix-Marseille Université and Institut Paoli-Calmettes, Parc Scientifique et Technologique de Luminy, 163 Avenue de Luminy, 13288 Marseille, France.
Email: juan.iovanna@inserm.fr

Abstract

Non-alcoholic fatty liver (NAFL) and related syndromes affect one-third of the adult population in industrialized and developing countries. Lifestyle and caloric oversupply are the main causes of such array of disorders, but the molecular mechanisms underlying their etiology remain elusive. Nuclear Protein 1 (NUPR1) expression increases upon cell injury in all organs including liver. Recently, we reported NUPR1 actively participates in the activation of the Unfolded Protein Response (UPR). The UPR typically maintains protein homeostasis, but downstream mediators of the pathway regulate metabolic functions including lipid metabolism. As increases in UPR and NUPR1 in obesity and liver disease have been well documented, the goal of this study was to investigate the roles of NUPR1 in this context. To establish whether NUPR1 is involved in these liver conditions we used patient-derived liver biopsies and in vitro and in vivo NUPR1 loss of functions models. First, we analyzed NUPR1 expression in a cohort of morbidly obese patients (MOPs), with simple fatty liver (NAFL) or more severe steatohepatitis (NASH). Next, we explored the metabolic

roles of NUPR1 in wild-type (*Nupr1*^{+/+}) or *Nupr1* knockout mice (*Nupr1*^{−/−}) fed with a high-fat diet (HFD) for 15 weeks. Immunohistochemical and mRNA analysis revealed NUPR1 expression is inversely correlated to hepatic steatosis progression. Mechanistically, we found NUPR1 participates in the activation of PPAR-α signaling via UPR. As PPAR-α signaling is controlled by UPR, collectively, these findings suggest a novel function for NUPR1 in protecting liver from metabolic distress by controlling lipid homeostasis, possibly through the UPR.

KEYWORDS

lipotoxicity, NAFL, NASH, NUPR1, PPAR-a signalling, UPR

1 | INTRODUCTION

The mechanisms underlying energy homeostasis have evolved to face periods of nutrient scarcity intermixed by periods of energy abundance. Obesity is a major concern for public health as it contributes to a variety of metabolic diseases including fatty liver disease, cardiovascular diseases, insulin resistance, type II diabetes.[1,2] Non-alcoholic fatty liver (NAFL) is an important metabolic condition that could lead to non-alcoholic steatohepatitis (NASH), cirrhosis and, ultimately, hepatocellular carcinoma.[1,3,4] Evidence suggests that endoplasmic reticulum (ER) stress, oxidative damage, mitochondrial dysfunction, and chronic inflammation contribute to the progression from NAFL to NASH and no effective treatment has been identified that slows down or reverses NASH progression.[1,4,5]

The ER stress response is an important signaling pathway for cell survival and adaptation to a range of cellular stresses including metabolic stress. In response to ER stress, the unfolded protein response (UPR) is rapidly activated.[6] The UPR activation allows for maintenance of protein homeostasis and restoration of ER functions[7,8] and recently it has been implicated in the regulation of hepatic lipid homeostasis.[9,10]

Nuclear protein 1 (NUPR1, p8, Com1) is a stress-induced protein that represents an intriguing link between cellular and ER stress. Initially discovered during the acute phase of pancreatitis[11-13] NUPR1 expression rapidly increases in all organs following exposure to stress and HFD.[14,15] Moreover, we recently reported that it is involved in the UPR activation[16] and in the regulation of lipid metabolism in hepatoma cells[17] and possesses a protective role against type II diabetes.[18] Yet NUPR1 functions in the context of HFD remain largely unexplored.

Since NUPR1 protects against significant tissue damage and affects acute UPR activation, we want to investigate the importance of NUPR1 in the context of metabolic disorders. By patient-derived biopsies and NUPR1 loss of function models, we showed that NUPR1 expression

Highlights

- NUPR1 protects liver from high caloric intake hepatic damage as it is inversely correlated with steatosis grade.
- NUPR1 participates in the regulation of lipid metabolism possibly through UPR and PPARα activation.
- Higher expression of NUPR1 was found in NAFL compared to NASH patients

inversely correlated to hepatic damage. We also unveiled an active role of NUPR1 in lipid metabolism and dyslipidemia during stress induced by HFD. Altogether, our data demonstrate that NUPR1 exerts a protective role in hepatocytes limiting lipotoxic injury.

2 | MATERIALS AND METHODS

2.1 | Tissue specimens and patients' characteristics

Fifty liver tissue samples from morbidly obese patients (MOPs) with NAFLD (n = 32) or NASH (n = 18) undergoing bariatric surgery were obtained from the Division of Surgery at the University Medical School of Palermo. As controls, we used histologically normal liver tissue obtained from biopsies (n = 6) performed in areas adjacent to the focal hepatic lesions of six patients whose liver metabolic parameters were in the normal range of values.

The study was approved by the Ethics Committee as spontaneous study No. 7/2014, which included male and female patients over 18 years old with Body Mass Index (BMI) $\geq$ 35 kg/m^2. Patients presenting with cirrhosis, Hepatocarcinoma (HCC), and liver steatosis caused by

mixed etiology, such as chemical exposure, were excluded from the study. All patients approved and signed consent to participate in the study. Before surgery, fasting blood samples were collected to evaluate serum levels of glucose, total cholesterol, triglycerides and HDL, alanine aminotransferase (ALT), aspartate aminotransferase (AST), gamma-glutamyl-transferase (GGT), total bilirubin, glycosylated hemoglobin A1c (HbA1c), and insulin. After surgery liver biopsies were assessed for steatosis, ballooning, and lobular inflammation by pathologists using the Kleiner classification system, and NASH was diagnosed using a NAFLD activity score $\geq$ 5. Liver biopsies were paraffin-embedded for immunohisto-chemistry analyses or snap-frozen and stored at $-80°C$ for RNA extraction and gene expression analyses (32 out of 50 patients). Anthropometric and clinical-pathological characteristics of MOPs are summarized in Table S1.

2.2 | Immunohistochemical analyses

For immunohistochemical analyses, tissue sections were deparaffinized and incubated with NUPR1 antibody diluted 1:200. Intensity of staining for nuclear and cytoplasmic NUPR1 was evaluated by pathologists. Staining intensity was evaluated as: 0 (no staining), 1 (low), 2 (moderate), and 3 (strong). Sum of nuclear and cytoplasmic intensity of NUPR1 was used to evaluate NUPR1 expression in all patients as a score ranging from 0 to 6.

2.3 | Human liver RNA extraction and qPCR

Thirty-two snap-frozen liver samples obtained from bariatric patients included in this study were first homogenized in liquid nitrogen and then total RNA extracted using Trizol reagent (#15596026, Thermo Fisher) according to the manufacturer's instructions. Total normal liver RNAs were obtained from five donors pool (BioChain, Newark, CA) and from four donors pool (Takara BioUSA, Mountain View, CA, USA). Three micrograms of total RNA were used for reverse transcription to obtain cDNA and real-time PCR was performed. mRNA expression level was evaluated using specific QuantiTect Primer Assays (QIAGEN) specific for *NUPR1* (QT00088382), *PPAR-α* (QT00017451), *PPAR-γ* (QT00029841), *SREBP1* (QT00036897), *FASN* (QT00014588), or *CPT1α* (QT00082236) were used. Expression level of *β-actin* (QT00046088) was used as an internal control. Each sample was analyzed in triplicate and data expressed as Log fold change calculated by the comparative cycle threshold Ct method ($2^{-\Delta\Delta Ct}$). qPCR conditions were as follows: 2 minutes at 94°C, 40 cycles of 5 seconds at 94°C and 10 seconds at 60°C.

2.4 | *Nupr1^{-/-}* and *Nupr1^{+/+}* mice

Nupr1^{-/-} mice bearing a homozygous deletion of exon 2 were used between 5 and 16 weeks of age. Control wild-type littermates are referred to as *Nupr1^{+/+}*. Animals were housed in the experimental animal house of the Centre de Cancérologie de Marseille (CRCM) of Luminy. All experimental procedures were approved by the *Comité d'éthique de Marseille numéro 14a* in accordance with EU regulations for animal experimentation.

2.5 | High-fat diet

Nupr1^{+/+} and *Nupr1^{-/-}* between the age of 5 and 6 weeks were fed on a normal chow diet (ND, 5.1% fat, SAFE diets #U8400G10R) or a High-Fat Diet 60% (HFD: Special Diet Services #824054; 20% protein, 60% fat, 20% carbohydrates) for 10 or 15 weeks with ad libitum access to food and water. During this time, weekly food was measured by monitoring the weight of the remaining food in the cage. Mice were weighed twice a week and sacrificed after 10 to 15 weeks by cervical dislocation. The liver was removed and immediately frozen in cold isopentane for long-term storage at $-80°C$, embedded in OCT or fixed in 10% formalin. Before sacrifice, blood was collected by submandibular bleeding (max. 0.25 mL), centrifuged at 14 000 rpm at 4°C, and *sera* were collected for further analysis.

2.6 | Histology

Liver samples were fixed in 10% formalin for 48 hours. Tissue was embedded in paraffin and 7 μm-thick sections stained with routine hematoxylin and eosin (H&E) for morphological analysis. Oil Red O was performed on 8 μm-thick cryosections, which were fixed (10% formalin) and then neutral lipids stained with Abcam Oil red O stain kit (#ab150678).

2.7 | Transmission electron microscopy

Mice were perfused with 4% cold PFA and 2.5% glutaraldehyde. Liver was cut into 1 mm^3 cubes and immersed overnight in 0.1 M Sorensen buffer, post-fixed in 1% osmium tetroxide, and en bloc stained with 3% uranyl acetate. The tissue was dehydrated with increasing concentrations of ethanol on ice and acetone before being embedded in Epon. Ultrathin sections (70 nm) were prepared using a Leica UCT Ultramicrotome (Leica, Austria) and stained with uranyl acetate and lead citrate. After contrasting, ultrathin sections were deposited on formvar-coated slot grids. The grids were

THE FASEB JOURNAL

observed in an FEI Tecnai G2 at 200 KeV and acquisition was performed on a Veleta camera (Olympus, Japan).

2.8 | Preparation of protein lysates and Western blotting

Tissue (40 mg) was lysed in ice-cold radioimmunoprecipitation assay (RIPA) buffer containing 0.5 µg/g of protease inhibitor kit (Sigma), 200 µM of Na_3VO_4, 1 mM of PMSF, and 40 mM of β-glycerophosphate. After homogenization with Precellys (Bertin Instruments) the supernatant was cleared by centrifugation for 30 minutes at 14 000 rpm (4°C). Protein content was quantified by micro BCA assay (Thermo-Fisher Scientific) and equal amounts of protein resolved by 5%-20% SDS-PAGE and blotted to a nitrocellulose membrane. Proteins were detected with specific primary antibodies (Table S2) and revealed with horseradish peroxidase conjugated secondary antibodies using enhanced chemiluminescence (ECL).

2.9 | Mice liver RNA extraction and real-time PCR

RNA was extracted from liver tissue using TRIzol reagent and RNA quality assessed with an RNA Nano Chip kit (Agilent) on an Agilent Bioanalyzer. Samples were treated with DNase using the RNase-free DNAse set (Qiagen). One microgram of total RNA from each sample was used to synthesize the first-strand cDNA by the GO-Script kit (Promega) and the provided oligo-dT following manufacturer's instructions. Quantitative PCR reaction was performed with primers listed in Table S3 and GoTaq qPCR master mix kit (Promega), using the Ariamx Real-time system (Agilent). Differential expression was calculated in relation to ribosomal phospho-protein P0 (*RPL0*), a reference gene transcript standard. All primers were synthesized by MWG.

The cycling parameters for the qPCR reaction included 40 cycles of denaturation at 95°C for 30 seconds, annealing at 62°C for 60 seconds, and elongation at 72°C for 30 seconds. Specificity of qPCR was established by incorporating non-reverse transcribed RNA. The specificities of the amplified transcripts were confirmed by melting curve profiles generated at the end of the PCR program.

2.10 | Measurement of ALT and AST activity in mice serum

Blood was collected from the mice in each group and serum separated by centrifugation. ALT and AST activity were measured with kits from Sigma (#MAK052 and #MAK055, respectively, Sigma-Aldrich) following the supplier's instructions.

2.11 | Measurement of liver triglycerides

Liver triglyceride content was measured using a Triglyceride Colorimetric Assay Kit from Cayman Chemical (#10010303) following the supplier's instructions.

2.12 | Cell line and in vitro experiments

Human hepatoma cells Huh7 were cultured in Dulbecco's Modified Eagle's Medium (DMEM; EuroClone, Milan, Italy) supplemented with 10% FCS (Gibco, Milan, Italy), 1 mM Sodium Pyruvate (Sigma-Aldrich, USA), 1 mM GlutaMAX (LifeTechnologies, Milan, Italy), and 1 mM penicillin-streptomycin (EuroClone, Milan, Italy) and maintained at 37°C and 5% CO^2. Cells were maintained at low passages and routinely tested for mycoplasm contamination and authenticated by short tandem repeat (STR) profiling (BMR Genomics, Padua, Italy). Free fatty acids-BSA and Sodium Palmitate used for in vitro induction of lipid accumulation were purchased from Sigma.

For *NUPR1* gene silencing, cells were cultured in the normal culture medium without antibiotics for 24 hours. Then cells were transfected as previously reported, using human *NUPR1* gene-specific siRNA (siNUPR1) and a control siRNA (siCTRL).[17] Twenty-four hours after transfection, cells were treated for 48 hours with two different doses (0.1 and 0.2 mM) of BSA-conjugated palmitic acid (PA) in DMEM high glucose supplemented with 1% of BSA, 1 mM GlutaMAX, and 1 mM of antibiotics. Cells treated only with BSA were used as control.

For BODIPY staining after PA treatment, cells were washed twice in PBS and fixed in 4% paraformaldehyde (PFA) for 20 minutes at room temperature. After fixation, cells were washed twice in PBS and stained with 0.5 µg/mL of BODIPY 493/503 (Sigma) for 5 minutes at room temperature, protected by light. After staining and washing cells in PBS, coverslips were mounted using VECTASHIELD, as mounting medium, containing DAPI to visualize nuclei. Images were acquired and collected at 40X magnification using a Leica microscope. Quantification of lipid droplets associated with green fluorescence was performed using ImageJ software and was expressed as green fluorescence area ($pixels^2$).

2.13 | Statistics

Statistical comparisons were performed using GraphPad Prism. For data obtained from MOPs-deriver liver sections, comparison between two groups (NAFL and NASH) were performed using a Mann-Whitney's non-parametric test. Data were reported as median ± interquartile range (IQR). Pearson's correlation analysis was used to evaluate the correlation of NUPR1 expression with clinicopathological characteristics of MOPs and with the expression of other genes. Spearman rank's correlation analysis was

performed to study the correlation between discrete variables, such as NUPR1 expression evaluated by IHC and steatosis severity. For mouse analysis, comparisons between two groups were performed using two-tailed unpaired Student's t tests. Comparisons involving two factors (usually diet and genotype) were performed with two-way ANOVAs and Sidak's post hoc corrections (Prism, GraphPad, USA). Data are reported as means ± SEMs. Results were considered significant with $P < .05$.

3 | RESULTS

3.1 | NUPR1 expression is inversely correlated to Kleiner steatosis grade

The mRNA expression levels of NUPR1 were evaluated by qPCR in liver biopsies from 32 morbidly obese patients (MOPs)

and as controls, we used histologically normal liver tissue obtained from biopsies of areas adjacent to the focal hepatic lesions (Figure 1). Results revealed higher expression of *NUPR1* mRNA in NAFL compared to NASH patients ($P = .0004$, Mann-Whitney's test, Figure 1B). Immunohistochemical analysis (IHC) of human biopsies (Figure 1C-E) were consistent with this observation. Livers from NAFL subjects contained more NUPR1-positive cells compared to NASH subjects (Figure 1D-F, black arrows and quantification, Mann Whitney, $P = .05$) Steatosis was next evaluated and ranked with Kleiner grade as previously reported[19] from low (0) to high (3). Spearman rank's correlation was then used to pair steatosis grade with NUPR1's expression in nuclei and cytoplasm (Figure 1G, Mann Whitney, $P = .006$). We also observed that hepatic NUPR1 mRNA expression inversely correlates with hepatic steatosis grade ($r = -.372$, $P < .05$ and $r = -.386$, $P < .001$, respectively, Figure 1H).
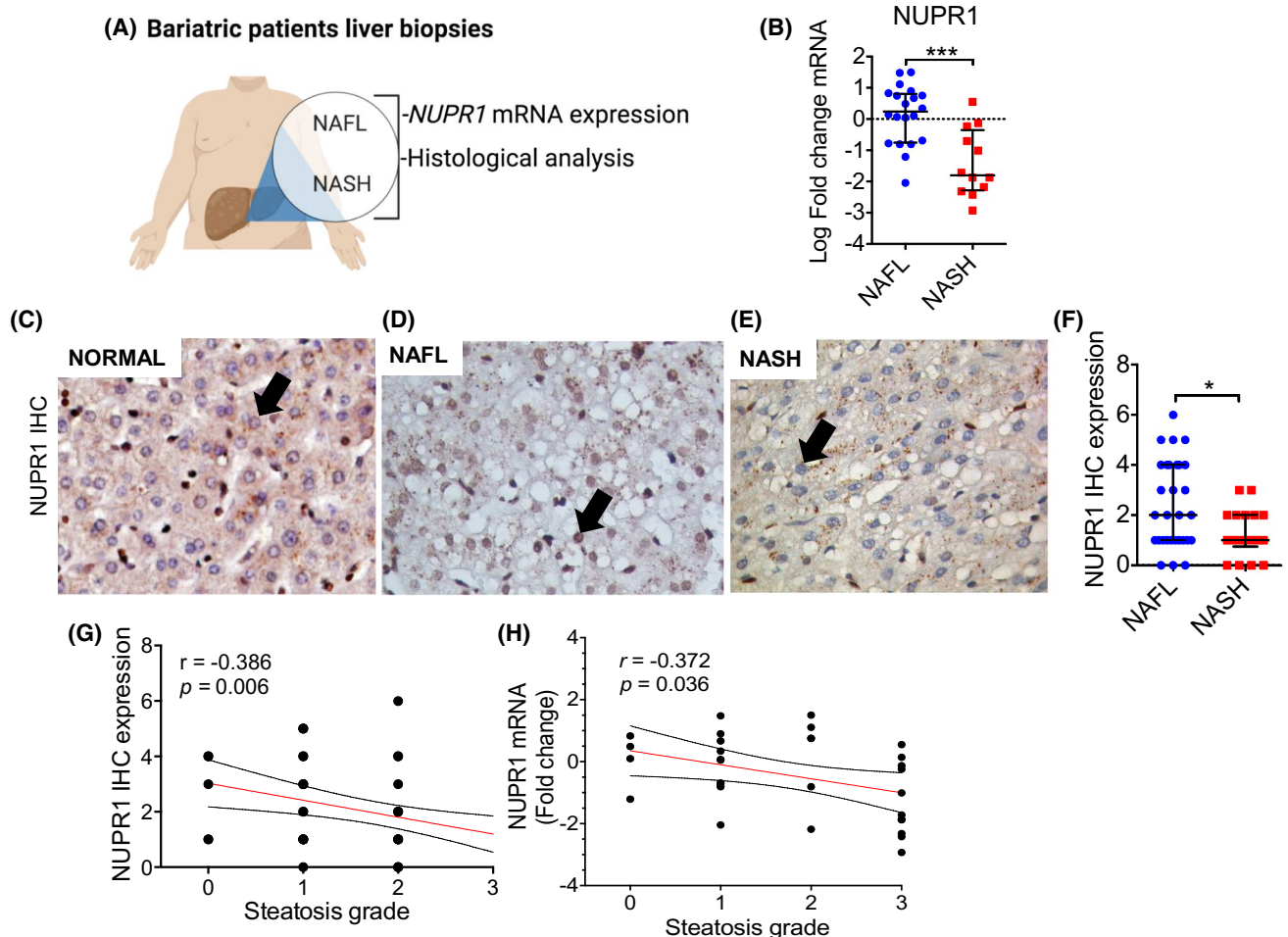

FIGURE 1 NUPR1 expression is inversely correlated to Kleiner steatosis grade. A, Expression of NUPR1 was evaluated in morbidly obese patients (MOPs) with histologically established non-alcoholic fatty liver (NAFL) or non-alcoholic steatohepatitis (NASH). B, qPCR analysis performed from liver of 32 MOPs with NAFL (n = 20) or NASH (n = 12). C-E, Representative images of NUPR1 protein expression evaluated by IHC in normal liver (n = 6) and in 50 MOPs with NAFL (n = 32) and NASH (n = 18). F, Differential expression of NUPR1 protein (expressed as the sum of nuclear and cytoplasmic protein intensity) between patients with NAFL (n = 32) and NASH (n = 18). G, Spearman's correlation between NUPR1 IHC cytoplasmic and nuclear expression and steatosis. H, Spearman's correlation between NUPR1 mRNA and Kleiner steatosis grade in MOP

A Pearson's correlation analysis between NUPR1 expression and several parameters used to characterize the patient cohort revealed that the lower the expression of NUPR1, the higher the hepatic damage (Table 1). High levels of NUPR1 were also associated with low serum levels of alanine transaminase (ALT) and aspartate transaminase (AST), two important markers of hepatic damage ($r = -.352$; $P = .023$ and $r = .353$; $P = .016$ for ALT and AST, respectively). Furthermore, NUPR1 expression positively correlated with serum level of high density lipoprotein (HDL) ($r = .350$; $P = .023$), a serum marker with well documented athero-protective role, anti-oxidant and anti-inflammatory activities,[20] (Table 1). Overall, these data suggest that NUPR1 may have a protective role in human progression from NAFL to NASH, since its expression is associated with lower levels of hepatic damage.

3.2 | *Nupr1*$^{-/-}$ mice are sensitized to hepatic damage in response to a high-fat diet

We previously reported that the germline deletion of NUPR1 generated phenotypically healthy, fertile mice that have lower resilience to stress injury.[12,21] To determine if NUPR1 expression has any role in the protective liver from lipotoxic injury we evaluated the response of *Nupr1* deficient animals to caloric excess using high-fat diet. Wild-type (*Nupr1*$^{+/+}$) and *Nupr1*$^{-/-}$ littermate mice were fed *at libitum* with a high-fat diet (HFD; 60% fat) or normal diet (ND; 5% fat) for up to 15 weeks (Figure 2A). The effect of HFD on the expression of *Nupr1* was evaluated by mRNA quantification with qPCR following 10 and 15 into HFD (Figure 2B). As expected, high-fat intake promoted an increase in the expression of

TABLE 1 Correlation between NUPR1 protein and clinical characteristics of morbidly obese patients

	r	*P*
Age	.097	.502
Gender	−.251	.078
BMI	−.253	.077
ALT	−.325	.023
AST	−.353	.016
GGT	−.134	.364
HDL	.350	.023
LDL	.062	.694
Total cholesterol	.179	.257
Triglycerides	−.130	.412
Blood glucose	−.177	.218
Insulin	−.166	.341
Hb1Ac	−.323	.042

Nupr1 mRNA levels in WT mice ($P < .0001$ and $P < .001$ for 10 and 15 weeks HFD, respectively).

Upon 10 weeks into HFD, mice gained significant weight compared to ND-fed mice ($P < .0001$, two-way ANOVA), but no significant difference in weight gain was registered between *Nupr1*$^{+/+}$ and *Nupr1*$^{-/-}$ mice (Figure 2C). Surprisingly, liver weight and gonadal fat resulted significantly higher in the *Nupr1*$^{-/-}$ group (Figure 2D,E).

Next, we assessed liver damage by measuring serum transaminase levels (Figure 2F). Serum levels of ALT were similar between ND-fed *Nupr1*$^{+/+}$ (15.04 ± 3.4 units/L) and *Nupr1*$^{-/-}$ mice (16.2 ± 2.7 units/L, $P > .99$). While ALT levels significantly increased in both genotypes with HFD ($P < .0001$, two-way ANOVA), *Nupr1*$^{-/-}$ mice showed significantly higher ALT levels compared to *Nupr1*$^{+/+}$ mice at both 10 weeks (64.3 ± 4.4 units/L vs 40.2 ± 8.4 units/L, respectively, $P = .02$), and 15 weeks (86.7 ± 5.0 units/L + 63.1 ± 8.0 units/L, $P = .02$). Similar results were obtained for AST serum levels. Again, AST serum levels were similar between ND-treated *Nupr1*$^{+/+}$ (23.3 ± 2.9 units/L) and *Nupr1*$^{-/-}$ (20.3 ± 2.8 units/L, $P = .97$) mice and significantly increased in both genotypes with HFD ($P = .0001$). While *Nupr1*$^{-/-}$ mice showed higher AST levels than *Nupr1*$^{+/+}$ mice at both 10 weeks HFD (46.3 ± 5.6 units/L vs 36.3 ± 4.9 units/L) and 15 weeks HFD (64.6 ± 7.4 units/L vs 49.1 ± 6.1 units/L), the difference reached statistical significance only at 15 weeks HFD ($P = .0175$). To determine if *Nupr1* deletion affected TG metabolism we compared TG levels in the different groups (Figure 2G). TG levels were similar between *Nupr1*$^{+/+}$ (37.8 ± 8.6 mg/g tissue) and *Nupr1*$^{-/-}$ (33.8 ± 6.1 mg/g tissue, $P = .9992$) mice under ND conditions. TG levels significantly increased in both genotypes with HFD ($P < .0001$) and once again, *Nupr1*$^{-/-}$ mice had higher TG levels than *Nupr1*$^{+/+}$ mice at both 10 weeks HFD (*Nupr1*$^{-/-}$ 232.3 ± 29.0 mg/g vs 115.1 ± 23.2 mg/g tissue, $P = .0085$) and 15 weeks HFD (295.2 ± 38.6 mg/g tissue vs 177.5 ± 30.3 mg/g tissue, $P = .008$).

Histological analysis on hepatic murine sections of *Nupr1*$^{+/+}$ or *Nupr1*$^{-/-}$ mice subjected to 10 or 15 weeks HFD was next evaluated. Characteristics of steatosis injury, including the appearance of presumptive lipid droplets and ballooning degeneration, were observed in both genotypes after 10 weeks HFD (Figure S1), being more pronounced in *Nupr1*$^{-/-}$ liver (Figure 3A,B). Of note, we observed limited areas free from fat accumulation around the periportal zone (Figure S1) in the absence of NUPR1. *Nupr1*$^{-/-}$ showed more severe mixed steatosis, characterized by lipid droplets of variable size (ranging from small to medium-sized, Figure 3A,B). At 15 weeks of HFD, *Nupr1*$^{-/-}$ mouse livers displayed severe macro-vesicular steatosis (>67% of macro-vesicular steatosis) with substantially increased numbers of lipid droplets. Additionally, *Nupr1*$^{-/-}$ hepatocytes showed
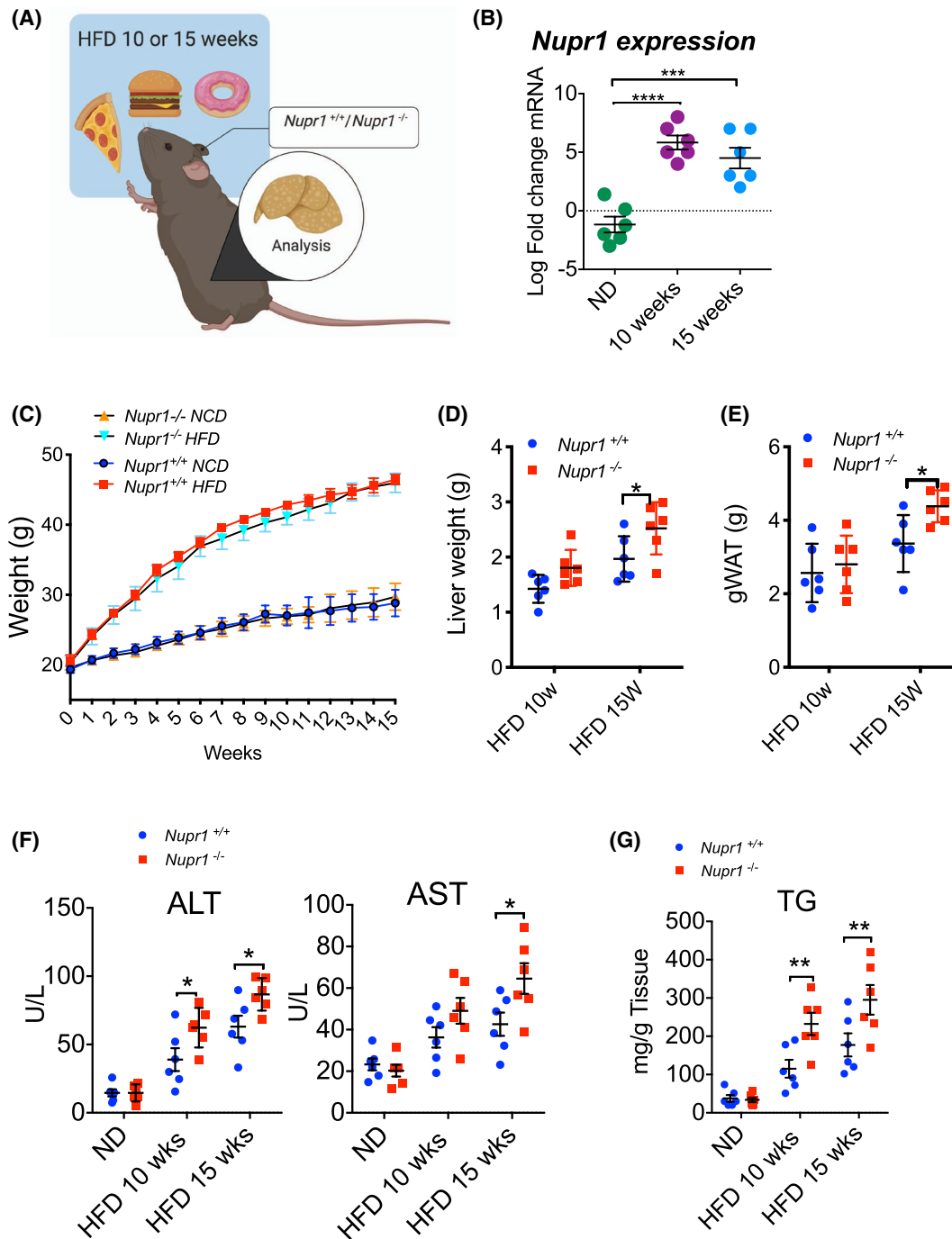
FIGURE 2 $Nupr1^{-/-}$ mice are sensitized to hepatic damage in response to a high-fat diet. A, $Nupr1^{+/+}$ and $Nupr1^{-/-}$ mice were fed for 10 or 15 weeks with high-fat diet fed regimen (60% FAT). B, Measure of $Nupr1$ mRNA levels after 10 or 15 weeks on HFD by qPCR. p values were calculated by two-way ANOVA with post hoc Sidak's test. Significant results are shown (****$P < .0001$ and ***$P < .001$ for 10 and 15 weeks HFD, respectively). Plotted data are means ± SEM, n = 6. C, Body weight increase compared to initial weight (%) after 10 and 15 weeks of HFD. D, Liver weight and (E) gonadal white adipose tissue (gWAT) resulted higher in the $Nupr1^{-/-}$ group. p values were calculated with two-way ANOVA with post hoc Sidak's test. Significant results are shown (*$P = .036$ for liver weight and *$P = .045$ for gWAT after 15 weeks HFD, respectively). F, Changes in serum circulating alanine aminotransferase (ALT) and aspartate transaminase (AST) were measure in livers from $Nupr1^{+/+}$ and $Nupr1^{-/-}$ after 10- or 15-weeks High-Fat or Normal Diet (ND). p values were calculated by two-way ANOVA with post hoc Sidak's test. Significant results are shown (*$P = .02$) Plotted data are means ± SEM, n = 6. G, Hepatic levels of triglycerides (TG) from $Nupr1^{+/+}$ and $Nupr1^{-/-}$ after 10 or 15 weeks HFD or ND. p values were calculated as above (**$P = .008$)

visibly severe hepatocytomegalia and wispy cytoplasmic elements, Mallory-Denk bodies (Figure 3B, black arrow and megamitochondria Figure 3B, arrowhead).

Ultrastructural analysis of liver sections by transmission electron microscopy (Figure 3C,D) showed a higher number of lipid droplets/cell in $Nupr1^{-/-}$ (65.3 ± 6.0) compared

to $Nupr1^{+/+}$ (40.5 ± 5.0, $P = .003$) and nuclear displacing (Figure 3C,D, black arrows). Nuclei displacement is another element characterizing hepatic injury derived from high caloric intake.[22]

3.3 | Silencing NUPR1 in Huh7 hepatoma cells promote lipid accumulation after palmitic acid treatment

To confirm the protective role of NUPR1 in the pathogenesis of liver steatosis we use a well-established in vitro model of lipid accumulation.[23,24] This involves the treatment of human hepatoma Huh7 cells with bovine serum albumin (BSA) conjugated to Palmitic Acid (BSA-PA conjugated) allowing cellular lipid uptake. Neutral lipids were next stained with BODIPY (493/503) and their accumulation was measured by fluorescence intensity (Figure 4A). Twenty-four h post-transfection, with $NUPR1$ gene-specific siRNA (siNUPR1) and a control siRNA (siCTRL), cells were treated for 48 hours with

0.1 and 0.2 mM BSA-PA conjugated. As expected, PA treatment stimulated NUPR1 mRNA expression in siCTRL cells (Figure 4B). Fluorescence analysis revealed that NUPR1 silencing promoted significantly higher accumulation of lipid droplets compared to control cells (Figure 4C,D), substantiating the role of NUPR1 in protecting cells from lipid accumulation and possibly, regulating the lipid metabolism.

3.4 | NUPR1 contributes to lipid homeostasis

Guided by histological and biochemical results, suggesting a protective role of $Nupr1$, we analyzed the expression of genes involved in lipid homeostasis (Figure 5). $Ppar$-α $Ppar$-γ and $Ppar$-δ, are key regulators of fatty acid oxidation and gluconeogenesis[25] and qPCR analysis revealed reduced activation in $Nupr1^{-/-}$ livers for $Ppar$-α ($P < .05$, $n = 6$) and $Ppar$-γ ($P < .001$, $n = 6$) after 10 weeks HFD feeding and, by 15 weeks, $Nupr1^{-/-}$ livers showed no increase in the expression of any $Ppar$-related
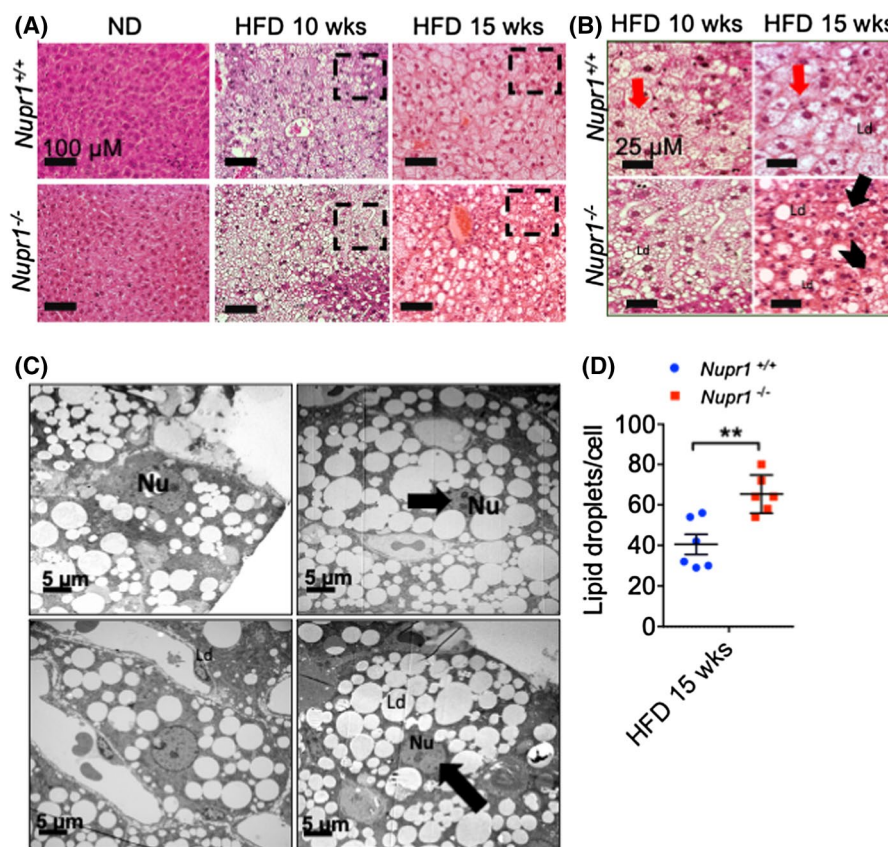

FIGURE 3 Histological analysis and electron micrographs of fatty liver revealed higher lipid accumulation in $Nupr1^{-/-}$ mice. A, Photographs of the hepatic section stained with hematoxylin and eosin to monitor fat accumulation after 10 and 15 weeks HFD. B, Cropped areas of histology sections from (A) (dashed square) Ld stands for lipid droplets; arrowheads indicate megamitochondria; black arrow indicates Mallory-Denk bodies. Scale bars are indicated in each image. C, Representative electron micrograph of perfusion fixed murine liver from wild type and $Nupr1^{-/-}$ after 15 weeks HFD showing fat droplets accumulation and nuclei displacing (black arrow). D, Quantification of lipid droplets in (C) was performed with ImageJ software. Unpaired Student's t test was used for statistical analysis (**$P = .003$)
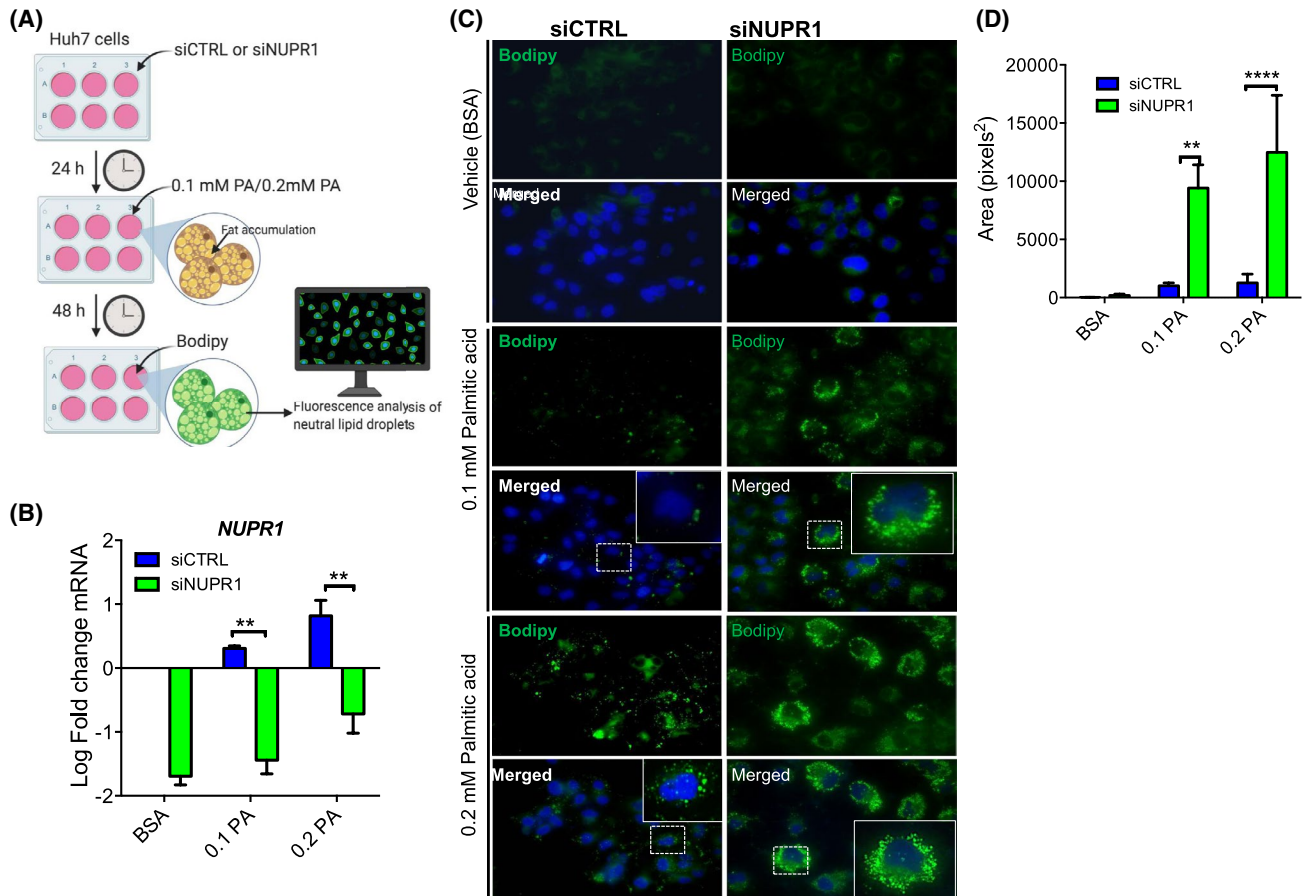
FIGURE 4 Genetically silencing of NUPR1 in Huh7 hepatoma cells promotes lipid accumulation after palmitic acid (PA) treatment. A, Human hepatoma cells, Huh7, were transfected for NUPR1 (siNUPR1) or with a control siRNA (siCTRL) and effects on lipid accumulation were evaluated after 48 hours of PA treatment. B, NUPR1 mRNA expression level in Huh7 cells (siCTRL and siNUPR1) expressed in Log Fold Change compared to treated cells for 48 hours with 0.1- and 0.2-mM PA. BSA- treated cells were used as control. Unpaired Student's t test was used for statistical analysis (N = 3). C, Representative images of BODIPY staining in Huh7 cells (siCTRL and siNUPR1) treated with 0.1 mM or 0.2 mM PA. Images were acquired at 40× magnification. D, Quantification of lipid droplets-associated green fluorescence was performed using ImageJ software and expressed as green fluorescence area (pixels^2). Two-way ANOVA with Post hoc Sidak's test was used to calculate statistical significance (**$P = .002$, ****$P < .0001$, n = 3)

genes analyzed compared to *Nupr1*$^{+/+}$. Analysis of genes involved in the regulation of lipid metabolism, including those involved in fatty acid oxidation and gluconeogenesis (*Pgc1α*) and lipogenesis (*Srebp1*-c and *ChreBP ChreBP*) showed similar results. In mice 10 weeks into HFD feeding, no significant differences were observed between *Nupr1*$^{+/+}$ or *Nupr1*$^{-/-}$ liver expression for *Pgc1α*, *Srebp1*-c or *ChREBP* (Figure 5A). By 15 weeks, differences in gene expression between *Nupr1*$^{+/+}$ and *Nupr1*$^{-/-}$ were statistically significant ($P < .05$ for *Pgc1α*, $P < .05$ for *Srebp1*-c and $P < .05$ for *ChREBP*). WB analysis confirmed lower protein expression of Ppar-α and Ppar-γ in *Nupr1*$^{-/-}$ mice fed 15 weeks HFD (Figure 5B,C).

To determine if reduced Ppar expression in *Nupr1*$^{-/-}$ mice was specific to PPAR signaling, similar analysis was performed for targets of *Ppar*-α translational activity (Figure 5D). These include *Fabp1* (fatty acid liver binding), *Cpt1α, Cpt1β, Mcad and Lcad* (fatty acid oxidation), and

Fasn (lipogenesis). Consistent with reduced PPAR signaling, all these genes, except *Fasn*, were expressed at lower levels in *Nupr1*$^{-/-}$ liver (Figure 5D). Collectively, data suggest that *Nupr1*$^{-/-}$ mice challenged with HFD have a reduced ability to activate genes involved in fatty acid oxidation, and this could result in accentuated steatosis and higher hepatotoxic damage compared to *Nupr1*$^{+/+}$ mice.

A similar analysis was next carried out in the cohort of MOPs (n = 32), and we correlated the expression of *SREBP1, FASN, PPAR-γ, CPT1α, and PPAR-α genes* to *NUPR1* mRNA levels. Consistent with our findings in mice, Pearson's correlation analysis showed that *NUPR1* mRNA expression correlated with increased expression of the analyzed metabolic genes (Figure 6A and Table 2). Conversely, patients classified as NAFL (n = 20) and NASH (n = 12) revealed NASH patients express lipid metabolism-related genes at significantly reduced levels (Figure 6B).
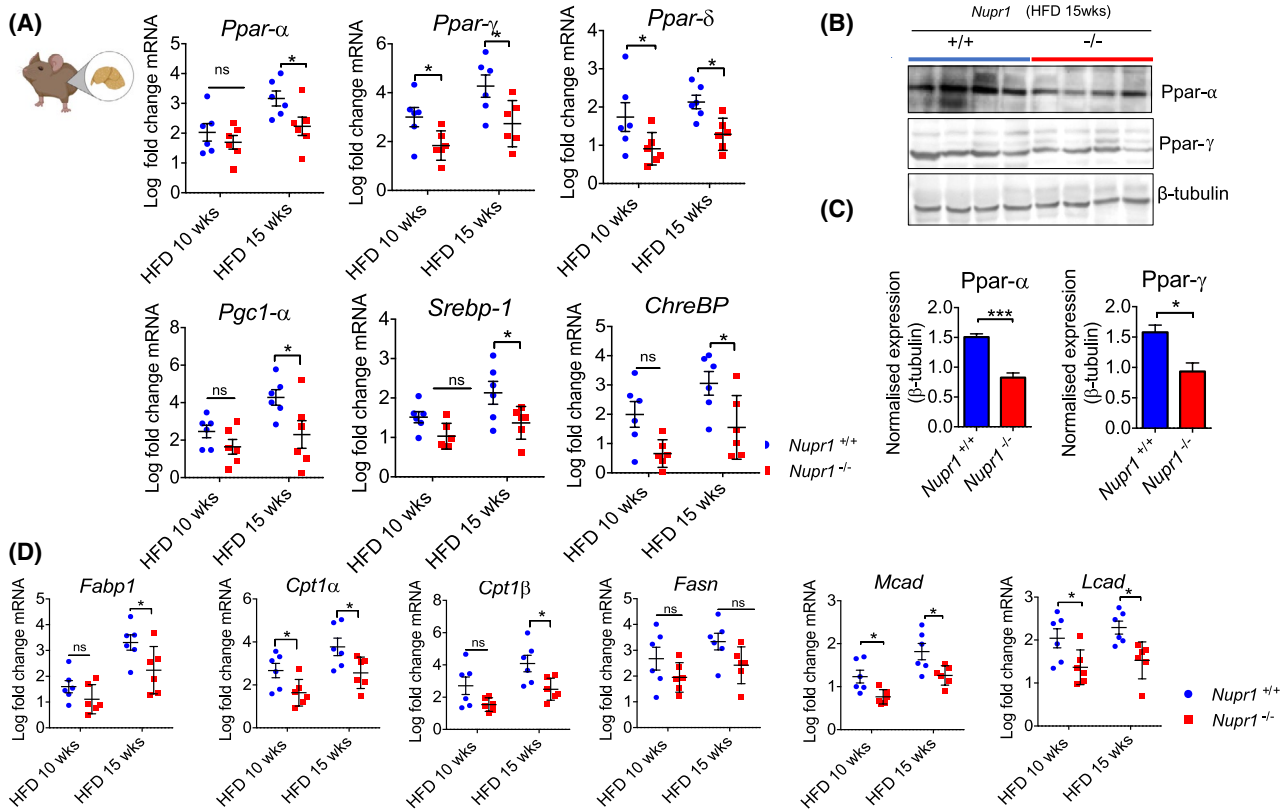
FIGURE 5 NUPR1 contributes to lipid homeostasis. A, RNA was prepared from liver dissected from *Nupr1⁺/⁺* and *Nupr1⁻/⁻* mice fed an HFD for 10 and 15 weeks. *Ppar-α, Ppar-δ, Ppar-γ, Pgc1-α Srebp-1,* and *ChREBP* mRNA were quantified relative to *Rpl0* by qPCR. N = 6. Data are presented as Log Fold Change compared to *Nupr1⁺/⁺* controls (fed a normal chow diet) levels of expression. Unpaired Student's t test was used for statistical analysis (*P = .04). B, Immunoblot of Ppar-α and Ppar-γ, and β-tubulin of tissue lysates prepared from livers dissected from wild-type and *Nupr1⁻/⁻* mice fed an HFD for 15 weeks. C, Quantification of (B) using ImageJ software. Mean band intensity plotted ± SEM (n = 4); unpaired Student's t test was used for statistical analysis (***P = .003 for PPar-α and *P = .01 for Ppar-γ). D, RNA was prepared from liver taken from *Nupr1⁺/⁺* and *Nupr1⁻/⁻* mice fed an HFD for 10 and 15 weeks. *Fabp1, Cpt1α* and *Cpt1β, Fasn, Mcad, Lcad* mRNA expression relative to *Rpl0* was quantified by qPCR, n = 6. Unpaired Student's t test was used for statistical analysis (*P = .01)

3.5 | Livers from *Nupr1⁻/⁻* mice exhibit a global reduction in the UPR response after 15 weeks of HFD feeding

Our results so far support a model in which reduced expression of NUPR1 in human and murine models is associated with the reduced ability to activate genes involved in lipogenesis and in lipid β-oxidation. As NUPR1 does not directly regulate gene expression, we examined pathways that may link NUPR1 to altered gene expression. NUPR1 has been linked to ER stress, which can promote pathology but also has an active role in regulating metabolic processes.[26] Therefore, the ER stress response was examined in *Nupr1⁻/⁻* livers in the context of HFD feeding (Figure 7). To do this, we assessed protein and mRNA expression for key mediators of the UPR branch. All protein levels were normalized to eIF2α levels of expression. Analysis of the PERK mediator ATF4 and its downstream target, CHOP, revealed significantly increased expression in response to 15 weeks of HFD treatment in *Nupr1⁺/⁺* liver tissue (0.4 ± 0.1 ND vs 0.8 ± 0.01 HFD, P = .0279 for

ATF4; 0.2 ± 0.07 ND vs 0.6 ± 0.07, P = .0091 for CHOP). *Nupr1⁻/⁻* mice on an ND showed no significant difference in ATF4 and CHOP accumulation relative to *Nupr1⁺/⁺* mice and also showed no significant increase in response to an HFD (Figure 7A and quantification D), suggesting defective activation of PERK signaling in the absence of NUPR1.

We next analyzed IRE1α and its mediator XBP1s (Figure 7B-F). WB analysis showed no significant difference between the two genotypes (basal levels (ND) or in response to HFD) for IRE1α expression. Conversely, while *Nupr1⁻/⁻* ND liver lysates tended to have higher levels of XBP1s compared to *Nupr1⁺/⁺* ND mice, the expression of XBP1s was only significantly increased in *Nupr1⁺/⁺* in response to HFD (P = .001). qPCR analysis confirmed activation of *Xbp1s* only in *Nupr1⁺/⁺* in response to HFD at 10 (1.3 ± 0.7 in *Nupr1⁺/⁺* vs 0.7 ± 0.1 in *Nupr1⁻/⁻*, P = .0104) and 15 weeks (2.2 ± 0.2 in *Nupr1⁺/⁺* vs 1.2 ± 0.2 in *Nupr1⁻/⁻*, P = .0077).

The analysis of ATF6 protein (Figure 7C) revealed higher expression in *Nupr1⁺/⁺* HFD samples (1.3 ± 0.2-fold increase) compared to *Nupr1⁺/⁺* ND mice (0.6 ± 0.07, P = .009) whereas,
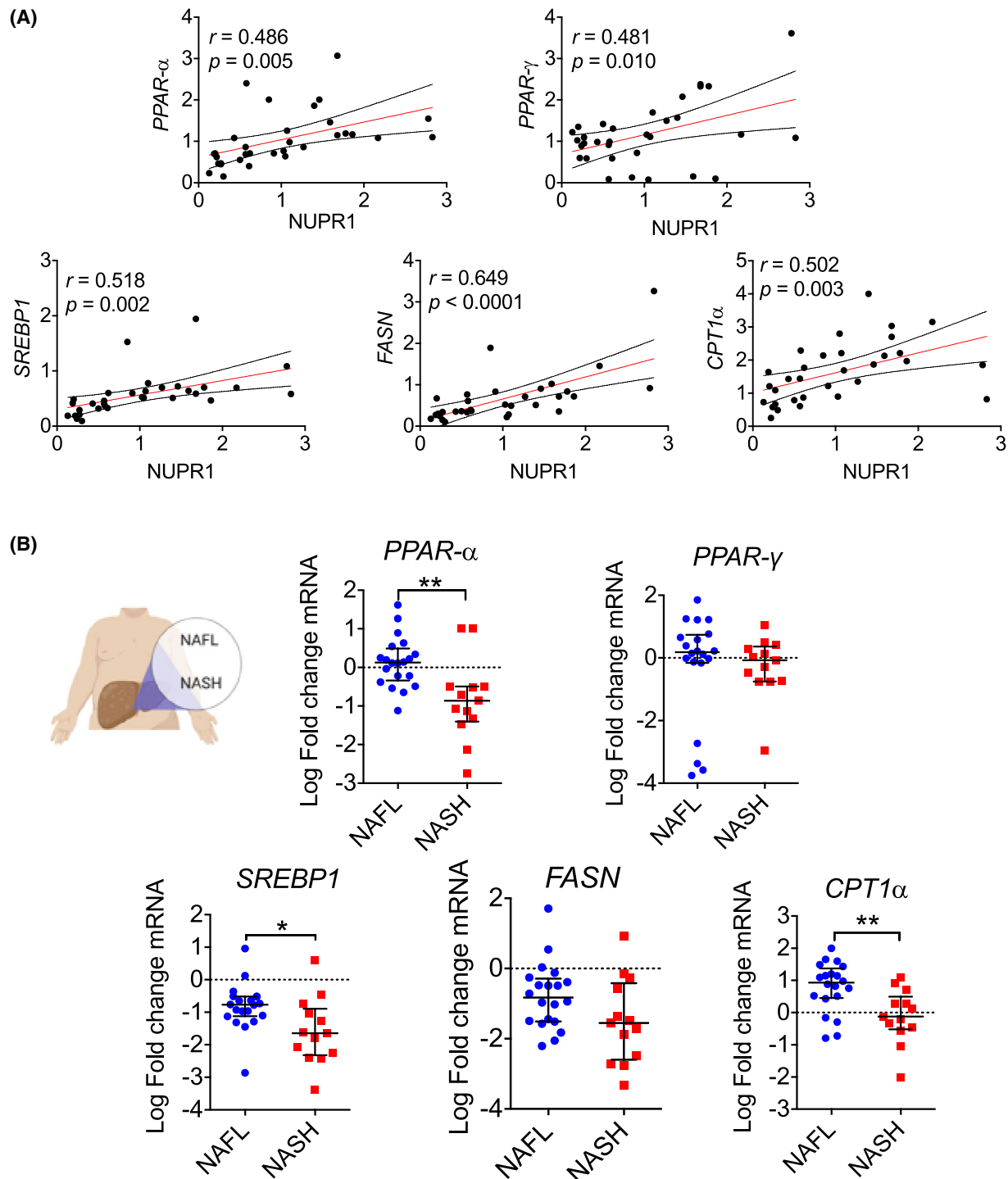
FIGURE 6 NASH patients have reduced activation of PPAR-α signalling. A, Pearson's correlation analysis between NUPR1 mRNA expression levels and expression of lipid metabolism-related genes in MOPs (n = 32). B, Expression of lipid metabolism-related genes in MOPs with NAFL (n = 20) or with NASH (n = 12). Data are expressed as Log Fold change compared to normal liver-derived RNA pools (n = 9). Mann-Whitney's non-parametric test was used for statistical significance. *$P < .05$; **$P < .01$

in the absence of *Nupr1*, the increase of ATF6 expression was not significant (0.4 ± 0.01 for ND vs 0.6 ± 0.08 after HFD feed, $P = .33$). qPCR confirmed a significant difference in *Atf6* expression between the two groups at both 10 weeks (1.5 ± 0.2 vs 0.5 ± 0.1-fold increase for *Nupr1*$^{+/+}$ and *Nupr1*$^{-/-}$, respectively, $P = .002$) and 15 weeks of HFD (2.6 ± 0.2 vs 1.2 ± 0.3

for *Nupr1*$^{+/+}$ and *Nupr1*$^{-/-}$ $P = .003$) (Figure 7G). Finally, the analysis of BiP/GRP78 expression, a key regulator of the UPR and downstream target for ATF6, showed no significant difference at protein levels between the two genotypes upon HFD (Figure 7C). In contrast, *BiP/Grp78* was significantly increased in *Nupr1*$^{+/+}$ (2.7 ± 0.2-fold relative to ND levels)

TABLE 2 Pearson's correlation between NUPR1 mRNA expression level and lipid metabolism-related genes in morbidly obese patients (n = 32)

	r	*P*
NUPR1 vs SREBP1	.518	.002
NUPR1 vs FASN	.649	<.0001
NUPR1 vs PPARγ	.448	.010
NUPR1 vs PPARα	.486	.005
NUPR1 vs CPT1α	.502	.003

compared to $Nupr1^{-/-}$ litter-mates (1.9 ± 0.1-fold relative to ND levels, $P = .005$) (Figure 7C,G). Altogether, these data indicate that the absence of NUPR1 reduces the activation of ER stress upon exposure to an HFD correlated to the disruption of hepatocytic lipid metabolism.

3.6 | Ultrastructural analysis of hepatocytes revealed the lack of evident ER ultrastructural alteration in the absence of Nupr1 after HFD feeding

To confirm altered the activation of the UPR in the absence of NUPR1, we studied the ultrastructure of hepatocytes using TEM, and focused or ER alterations induced in $Nupr1^{+/+}$ and $Nupr1^{-/-}$ by a 15-week HFD (Figure 8). Representative TEM images from $Nupr1^{+/+}$ and $Nupr1^{-/-}$ fed with ND revealed similar morphology. Mitochondria were readily apparent (white arrowhead), the ER was packed into long thin parallel tube-like structures (white arrows), and glycogen deposition was observed. Interestingly, hepatocytes of ND $Nupr1^{-/-}$ mice contained vacuole-like structures (compare Figure 8A,B, indicated by black arrows). At 15 weeks HFD, both $Nupr1^{+/+}$ and $Nupr1^{-/-}$ exhibited electron-dense protein aggregates inside the ER (Figure 8G,H; yellow arrows). Additionally, the ER in $Nupr1^{+/+}$ mice showed a disorganized structure compared to $Nupr1^{-/-}$ mice and expansion/dilation of ER-cisternae (Figure 8G; red asterisks), which are morphological signs of ER-stress. These changes were not observed in $Nupr1^{-/-}$, where hepatocytes displayed an ordered ER structure. These data confirm that in absence of NUPR1, activation of ER stress by fat oversupply is greatly reduced and could contribute to the increased hepatic injury observed in $Nupr1^{-/-}$ mice.

3.7 | Nupr1 deficient mice exhibit a dysfunctional lipid accumulation and unfolded protein response after Tunicamycin induced ER stress

So far, our data indicate that the absence of NUPR1 associates with a marked susceptibility to hepatic damage and

a general decrease in UPR activation following cell stress injury promoted by HFD. We wanted to verify next, if stressing the ER by pharmacological means could lead to similar results. To this end, we induced a pharmacological activation of the UPR in $Nupr1^{-/-}$ and $Nupr1^{+/+}$ mice with Tunicamycin (Tun) (Figure 9A), which induces ER stress by inhibiting N-Glycosylation and consequently correct protein folding.[27] Administration of ER stress-inducing chemical agents promotes hepatic steatosis in mice and although several mechanisms have been proposed, it is debated how ER stress promotes hepatic lipid dysregulation.[28,29]

Hematoxylin and eosin-stained liver sections of mice challenged with Tun showed lipid accumulation, which becomes more evident as time went by (Figure 9B). Height hours post injection, hepatocytes of $Nupr1^{+/+}$ and $Nupr1^{-/-}$ mice displayed cytoplasmic swelling. However, in $Nupr1^{+/+}$ the condition resulted milder compared to $Nupr1^{-/-}$ where swelling was also associated with more severe ballooning degeneration. A Kleiner score of 1/8 was attributed to $Nupr1^{+/+}$ slices (0 for steatosis, 0 for inflammation, 1 for ballooning) and a Kleiner score of 2/8 was assigned to $Nupr1^{-/-}$ slices (0 for steatosis, 0 for inflammation, 2 for ballooning.[19] At 24 hours $Nupr1^{-/-}$ liver section presented diffuse micro-vesicular steatosis in 90% of hepatocytes, whereas in $Nupr1^{+/+}$ hepatocytes were characterized by a more evident ballooning degeneration compared to the 8 hours samples without, however, the appearance of steatosis. A Kleiner score of 2/8 was assigned for $Nupr1^{+/+}$ slices (0 for steatosis, 0 for inflammation, 2 for ballooning), whereas a score of 5/8 (3 for steatosis, 0 for inflammation, 2 for ballooning) was attributed to $Nupr1^{-/-}$ slices, further substantiating the contribution of $Nupr1$ in protecting from NASH development.

We next examined the hepatic injury by measuring the serum levels of ALT, AST, and TG (Figure 9C,D). ALT levels resulted elevated in both genotypes when compared to control (8.2 ± 2.1 and 10.9 ± 2.0, $Nupr1^{+/+}$ and $Nupr1^{-/-}$ for controls vs 34.8 ± 2.9 and 45.9 ± 4.0 Tun treated, for $Nupr1^{+/+}$ and $Nupr1^{-/-}$, respectively) and multiple comparison using two-way ANOVA (with Sidak's test) revealed that $Nupr1^{-/-}$ showed higher levels (*$P = .043$, n = 6). Furthermore, AST serum levels were significantly increased in both genotypes after Tun compared to ND groups (23.3 ± 2.85 and 20.30 ± 2.83 for $Nupr1^{+/+}$ and $Nupr1^{-/-}$, respectively, for the controls and 37.3 ± 5.1 and 54.0 ± 5.4) and the levels resulted significantly higher in $Nupr1^{-/-}$ (analyzed with two-way ANOVA and corrected for multiple comparisons using Sidak test *$P = .02$, n = 6). Additionally, hepatic triglycerides resulted in 1.5-fold higher in $Nupr1^{-/-}$ Tun treated compared to $Nupr1^{+/+}$ counterpart (42.9 ± 4.3 and 64.9 ± 5.7 for WT and KO treated, respectively, ***$P = .001$, n = 6, two-way ANOVA analysis corrected for multiple comparisons with Sidak's test). We also compared the mRNA levels of
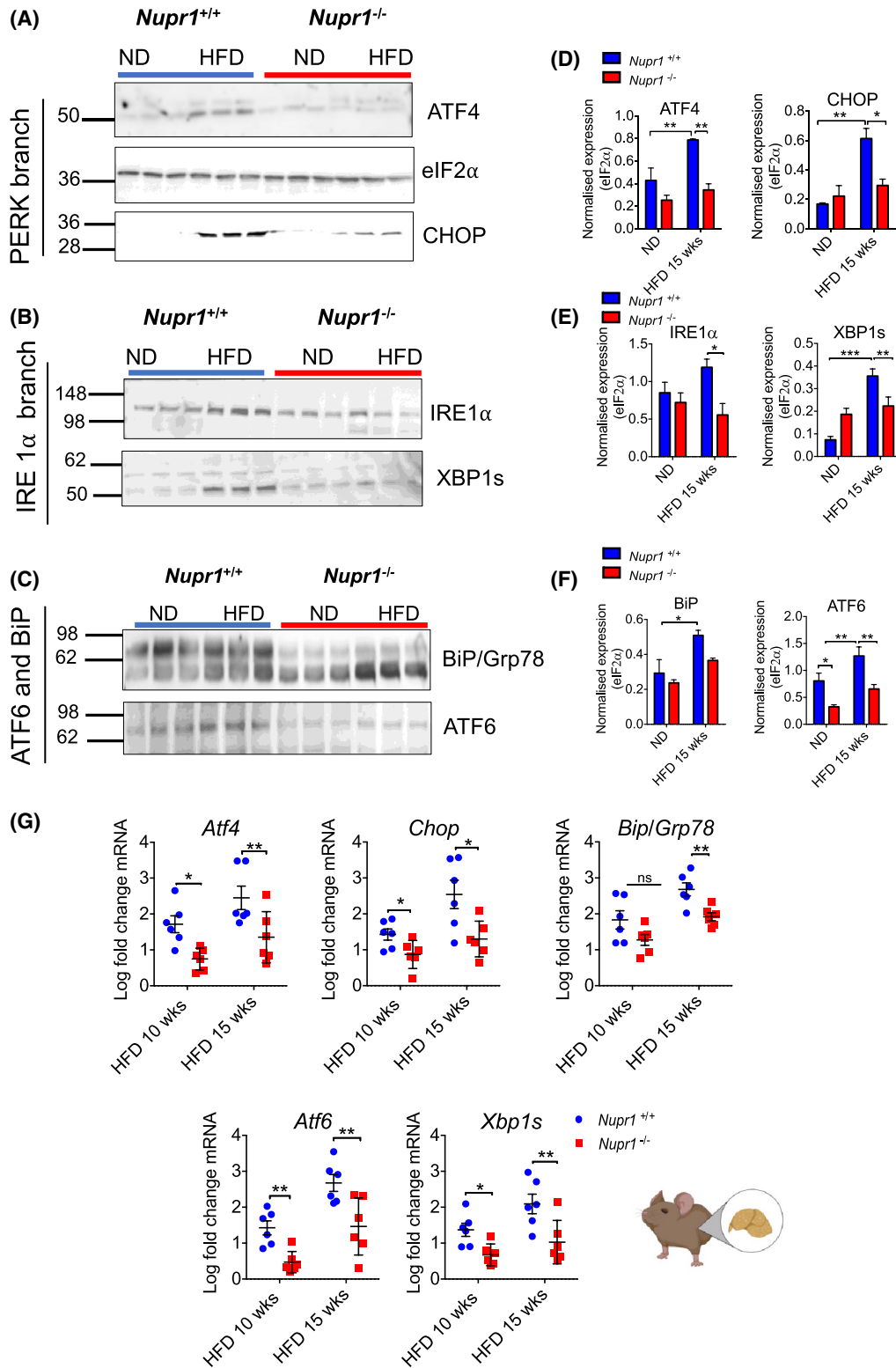
FIGURE 7 Livers from *Nupr1*^{−/−} mice exhibit a global reduction in the ER stress response after 15 weeks of HFD feeding. A-C, Western blot of ATF4, eIF2α, CHOP, IRE1α XBP1s, BiP, and ATF6, of tissue lysates prepared from livers dissected from wild-type and *Nupr1*^{−/−} mice fed an HFD for 15 weeks. D-F, Quantification of (A-C) using ImageJ software. Mean band intensity plotted ± SEM; Significant differences were calculated by two-way ANOVA with post hoc Sidak's test (*P = .04; **P = .03). G, qPCR results of mRNA expression of *Atf4, Chop,* BiP/Grp78, *Atf6, and Xbp1s.* RNA was extracted from *Nupr1*^{+/+} and *Nupr1*^{−/−} mice fed an HFD for 10 and 15 weeks and mRNA levels quantified relative to *Rpl0.* Mean plotted ± SEM. Unpaired Student's t test was used for statistical analysis (n = 6) (*P = .02; **P = .003)
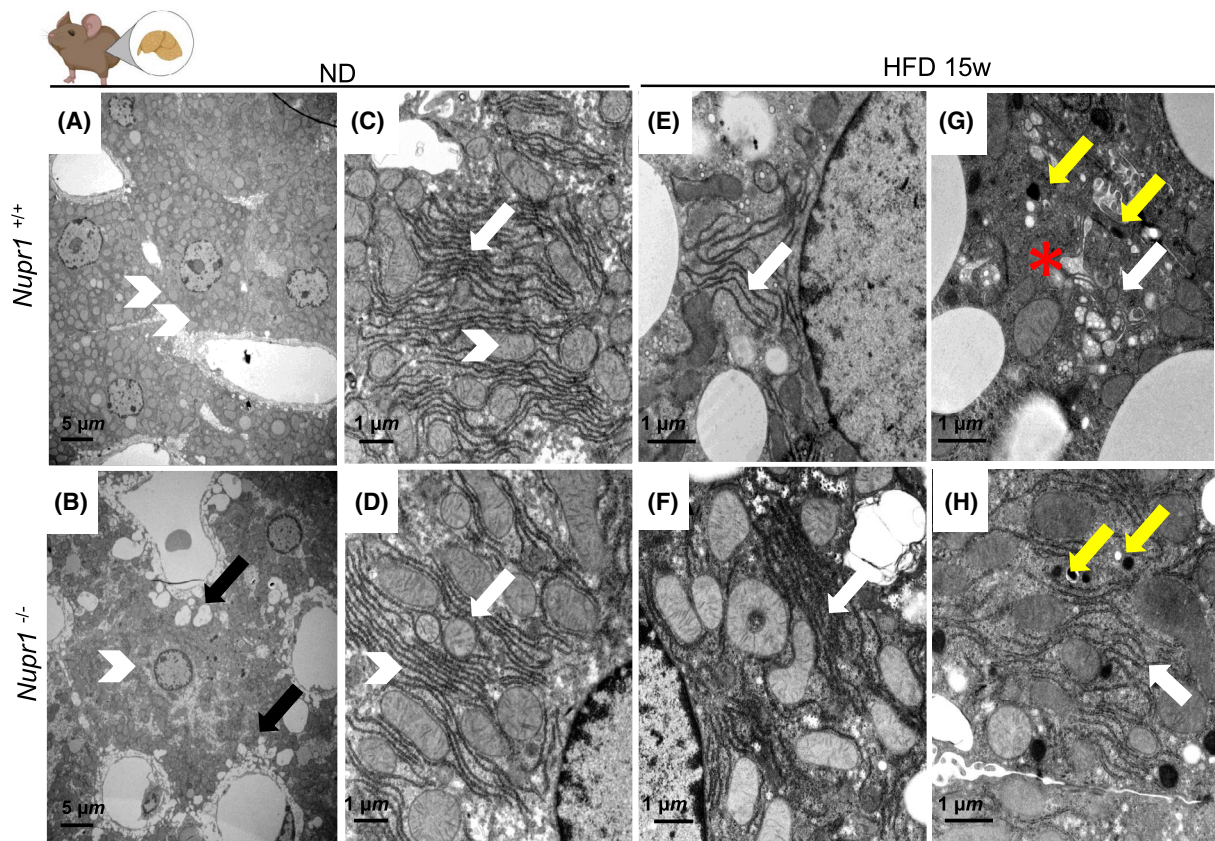
FIGURE 8 Electron micrographs of perfusion fixed mice upon HFD showed reduced signs of ER stress in absence of Nupr1. Representative micrographs of perfusion fixed mice liver ultrathin sections from *Nupr1*^{+/+} and *Nupr1*^{−/−} fed with Normal chow diet (A-D) or HFD for 15 weeks (E-H) are shown. A and B, ND samples; white arrowhead points toward ER and white arrow to mitochondria; black arrow points to vacuole like structure (B). C and D, higher magnification of ND liver sample. Yellow arrows in G and H indicate protein aggregates; red asterisk indicates ER expansion (G). White arrows in G and H indicate the differences in ER cisternae

the UPR downstream mediators Atf4, Chop, Xbp1s, BiP/Grp78, and Atf6 (Figure 9E). Similar to HFD, 8 hours of treatment with Tunicamycin led to a decreased activation of UPR mediators in deficient mice, further substantiating a role for NUPR1 in mediating UPR during cellular injury.

4 | DISCUSSION

NUPR1 is stress-activated protein rapidly expressed in response to acute stress events including sepsis and pancreatitis.[17,30-33] Recent studies suggest NUPR1 affects the ER stress response[16,34] contributing to hepatocarcinogenesis.[17] Since NUPR1 has been linked to oxidative stress and is required for a proper UPR activation under acute stress conditions, we wanted to examine NUPR1's role in a more clinically relevant form of liver damage. While elevated expression of NUPR1 in the context of high-fat diet has previously been reported,[14,15] its effects on the liver response to this form of chronic stress have not been examined.

The UPR maintains protein homeostasis through three pathways—PKR-like ER kinase (PERK), inositol-requiring

enzyme 1 (IRE1), and activating transcription factor 6 (ATF6).[35] PERK activation reduces translation through the phosphorylation of eukaryotic initiation factor eIF2α, while active IRE1 acts as an endonuclease by promoting the splicing of *Xbp1*. Intermembrane proteolysis during ER stress leads to ATF6 activation, which also promotes the expression of chaperones and BiP/GRP78. Hepatic deletion of *Xbp1s* decreased expression of lipogenic genes,[36,37] while attenuation of eIF2α activity protects from hepatic steatosis.[38] Germline deletion of *Ire1α* or *Atf6* results in abnormal accumulation of hepatic steatosis following high-fat diet (HFD) feeding[39] and dominant-negative or siRNA-mediated knockdown of *Atf6* increased susceptibility to hepatic steatosis by decreasing transcriptional activity of peroxisome proliferator-activated receptor α (PPAR-α;[40]). PPAR-α is highly expressed in the liver and plays a pivotal role in controlling lipid metabolism. Combined, these data strongly support a relationship between ER stress response and lipid metabolism. As NUPR1 is highly expressed following all sorts of cell injury and participate in UPR activation, within this work we wanted to shed light on a possible link between NUPR1, UPR activation, and lipid metabolism.
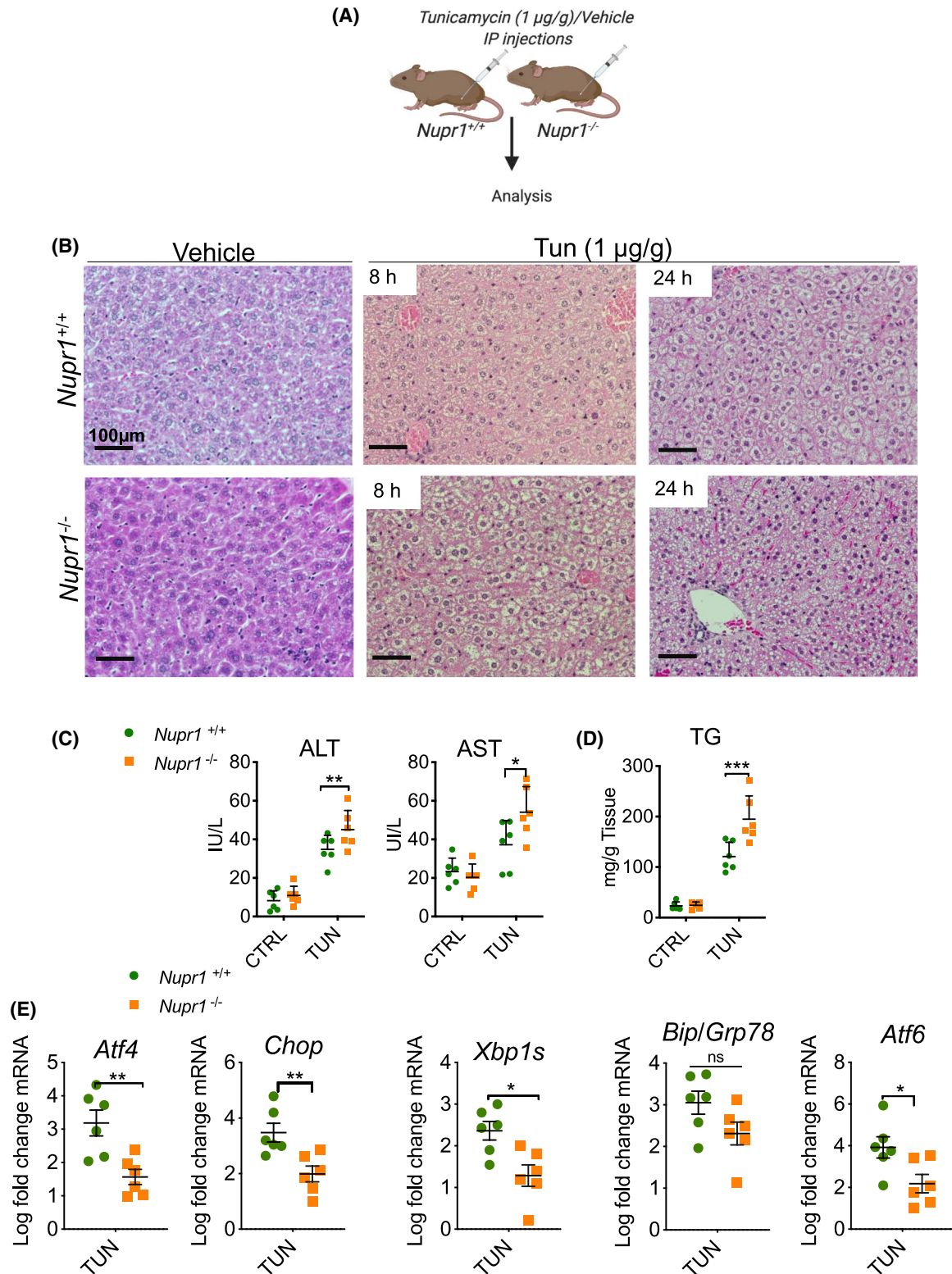
FIGURE 9 *Nupr1* deficient mice exhibit a dysfunctional lipid accumulation and incomplete unfolded protein response after tunicamycin induced ER stress. A, *Nupr1*$^{+/+}$ and *Nupr1*$^{−/−}$ mice were injected with 1 μg/g of Tunicamycin and after 8 or 24 hours post-injection liver and serum were collected. B, Photographs of the hepatic section stained with hematoxylin and eosin to monitor fat accumulation after Tun treatment. C, Changes in serum circulating alanine aminotransferase (ALT) and aspartate transaminase (AST) were measure in livers from *Nupr1*$^{+/+}$ and *Nupr1*$^{−/−}$ after 10- or 15-weeks High-Fat or Normal Diet (ND). p values were calculated by two-way ANOVA with post hoc Sidak's test. Significant results are shown (*P = .02) Plotted data are means ± SEM, n = 6. D, Hepatic levels of triglycerides (TG) from *Nupr1*$^{+/+}$ and *Nupr1*$^{−/−}$ after 10 or 15 weeks HFD or ND. p values were calculated as above (**P = .008). E, qPCR results of mRNA expression of *Atf4, Chop, Xbp1s*, BiP/Grp78, and *Atf6*. RNA was extracted from *Nupr1*$^{+/+}$ and *Nupr1*$^{−/−}$ mice IP treated with tunicamycin (1 μg/g) and levels quantified relative to *Rpl0*. Mean plotted ± SEM. Unpaired Student's t test was used for statistical analysis (n = 6) (*P = .01; **P = .004)
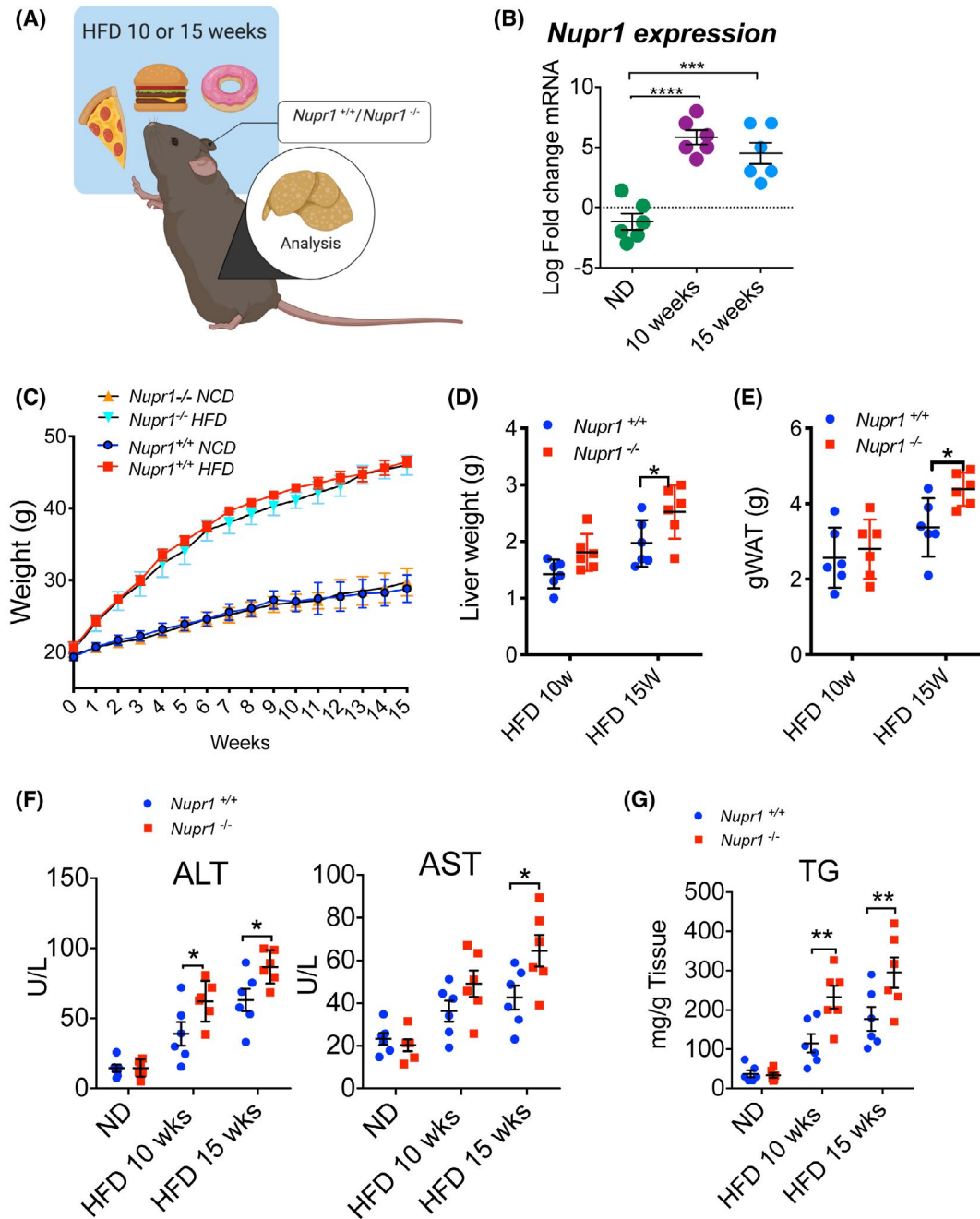
FIGURE 10 NUPR1 participates in the regulation of hepatic lipid metabolism possibly through a UPR dependant mechanism. NUPR1 participates in the activation of PPAR-α signaling possibly via UPR. Such events allow an increase in hepatic metabolism and consequently protection from lipotoxic injury

In both rodent and human samples, NUPR1 loss was associated with higher degree of steatosis and a more severe hepatic injury. The mechanism behind the phenotype appears to be associated with the improper activation of the PPAR-α signaling, a pathway involved in fat metabolism and particularly fatty acid oxidation. Our study suggests a link between NUPR1 and regulation of such pathway. PPAR-α signaling genes belong to a family of regulators associated with lipid metabolism, and include *Ppar*-α, which controls fatty acid Ppar-γ, *Pgc-1*, and *Srebp* genes, reprograms liver metabolic

mRNA expression, and participates in maintaining lipid homeostasis. All of these genes, including their targets (eg, *Fabp1 Cpt1α, Cpt1β, Fasn* and *Mcad,* and *Lcad)* are up-regulated by an HFD, but their upregulation is muted or attenuated in the absence of NUPR1.

The activation of PPAR-α coordinates fatty acid oxidation and is ultimately responsible for liver lipid homeostasis and energy balance. Negative regulation of PPAR-α signaling and the repression of its target genes impairs fatty acid oxidation and increases liver lipid deposit. However, it is possible that

NUPR1 directly targets metabolic genes. *Nupr1* is biochemically related to HMG-I(Y) proteins which promote architectural changes in the DNA and modulate gene expression[13,41] and participates in the modulation of several transcriptional programs. The observed data could be interpreted that the improper regulation of the UPR and metabolic gene expression are independent events.

While the data within this study suggests a link between NUPR1, improper regulation of the UPR and altered metabolic gene expression, a direct link between these events has remained elusive. It is possible that these events are independent. NUPR1 is rapidly expressed after injury, yet in these models, there is long-term exposure to increased dietary fat in the rodent model and a high degree of steatosis in the human samples. In both models, there is chronic stress and several studies show NUPR1 expression is intrinsically associated with ER-stress. Therefore, it could be possible that the disruption of ER-homeostasis is an upstream factor of NUPR1 malfunction and lower expression in human steatosic livers.

Yet, our data suggest that NUPR1 affects metabolic gene expression by altering the UPR during HFD as all three branches of the UPR are suppressed in the absence of NUPR1. In the liver, the UPR activation is associated with metabolic dysfunction derived from abnormal dietary demand. Several elements of the UPR play a direct role in regulating lipid metabolic pathways. Both ATF3 and ATF4, downstream mediators of PERK signaling, target metabolic genes,[42-44] and ATF6 can promote PPAR-α signalling.[40] We suggest that ATFs may directly regulates activity of PGC1a, a key transcription cofactor that, in turn, may activates PPAR-α. *Atf6* deficient mice are susceptible to tunicamycin-induced liver steatosis,[45] and we identified a similar requirement for NUPR1 in response to an HFD and ER-stress pharmacological activation. The expression of ER stress mediators is reduced in HFD *Nupr1*$^{-/-}$ livers compared to *Nupr1*$^{+/+}$ mice, which show significant increases in UPR activity and expression to HFD-treatment. ATF6 also directly interacts with PPAR-α and ATF6 inhibition represses the recruitment of PPAR-α to target gene promoters containing the PPRE element.[40]

Deficient activation of XBP1s is also observed in liver-specific *Ire1a* null mice, and leads to enhanced accumulation of fat in hepatocytes, suggesting a potential role for XBP1s in protecting liver form hepatic steatosis. The ability of XBP1s in acting as an anti-lipogenic is documented in two additional mouse models of obesity and NAFLD, and, increasing the activity of XBP1s reduced hepatic TG content. Accordingly, lack of XBP1s in the absence of *Nupr1* was associated with increased NAFLD phenotype, indicating that all three branches of the UPR can contribute to lipid metabolism in the liver.[46,47]

However, while our current study does not provide a direct link between NUPR1 and UPR in the liver, it strongly supports a model by which NUPR1 regulates hepatic lipid metabolism through a UPR-dependant manner. Further studies are warranted to identify the direct links between NUPR1 and lipid metabolism in the liver.

Altogether, our findings provide novel insight on NUPR1 function describing a putative mechanism by which stress-related proteins are involved in regulating lipid metabolism. As NUPR1 is being evaluated as a possible drug target for hepatocarcinoma and pancreatic ductal adenocarcinoma, care should be taken in monitoring liver parameters.

5 | CONCLUSION

In conclusion, we showed NUPR1 participates in the regulation of hepatic fatty acid and contributes to the control of lipid homeostasis, possibly through multiple branches of the UPR (Figure 10). These findings provide a novel insight by which NUPR1 is involved in regulates lipid metabolism and reinforce the idea that the modulation of the UPR and PPAR-α could be of particular interest in the development of therapies for metabolism-associated pathologies.

CONFLICT OF INTEREST
No conflict of interest to declare.

AUTHOR CONTRIBUTIONS
M. Teresa Borrello designed and performed all the mice experiments analyze and interpreted the data and wrote the manuscript; M. Rita Emma designed and performed the experiments on patient samples and wrote the manuscript; A. Listi performed the experiments under the supervision of M. Teresa Borrello; M. Rubis performed the rodent histology and S. Coslet helped with histological data interpretation; A. Cusimano and G. Pantuso performed in vitro experiments; D. Cabibi and R. Porcasi performed IHC analysis; M. Soresi gave his support for the statistical analysis of human-derived data; L. Giannitrapani and G. Montalto were involved in patient's enrolment; G. Pantuso provided surgical resections from morbidly obese patients; K. Blyth gave her support in data analysis and critical revision of the manuscript. C. Pin, M. Cervello, and J. Iovanna design the study, helped with the data interpretation, supervised M. Teresa Borrello and M. Rita Emma, and wrote the manuscript.

ORCID
Maria Teresa Borrello https://orcid.org/0000-0003-1365-1358

REFERENCES
1. Younossi Z, Anstee QM, Marietti M, et al. Global burden of NAFLD and NASH: trends, predictions, risk factors and prevention. *Nat Rev Gastroenterol Hepatol*. 2018;15:11–20.
2. Younossi ZM. Non-alcoholic fatty liver disease—a global public health perspective. *J Hepatol*. 2019;70:531-544.

3. Marra F, Gastaldelli A, Baroni GS, Tell G, Tiribelli C. Molecular basis and mechanisms of progression of non-alcoholic steatohepatitis. *Trends Mol Med*. 2008;14:72-81.

4. Michelotti GA, Machado MV, Diehl AM. NAFLD, NASH and liver cancer. *Nat Rev Gastroenterol Hepatol*. 2013;10:656-665.

5. Lebeaupin C, Vallée D, Hazari Y, Hetz C, Chevet E, Bailly-Maitre B. Endoplasmic reticulum stress signalling and the pathogenesis of non-alcoholic fatty liver disease. *J Hepatol*. 2018;69:927-947.

6. Schönthal AH. Endoplasmic reticulum stress: its role in disease and novel prospects for therapy. *Scientifica*. 2012;2012:857516.

7. Gupta S, McGrath B, Cavener DR. PERK regulates the proliferation and development of insulin-secreting beta-cell tumors in the endocrine pancreas of mice. *PLoS ONE*. 2009;4:e8008.

8. Harding HP, Zeng H, Zhang Y, et al. Diabetes mellitus and exocrine pancreatic dysfunction in perk$^{-/-}$ mice reveals a role for translational control in secretory cell survival. *Mol Cell*. 2001;7:1153-1163.

9. Wang M, Kaufman RJ. Protein misfolding in the endoplasmic reticulum as a conduit to human disease. *Nature*. 2016;529:326-335.

10. Han J, Kaufman RJ. The role of ER stress in lipid metabolism and lipotoxicity. *J Lipid Res*. 2016;57:1329-1338.

11. Mallo GV, Fiedler F, Calvo EL, et al. Cloning and expression of the rat p8 cDNA, a new gene activated in pancreas during the acute phase of pancreatitis, pancreatic development, and regeneration, and which promotes cellular growth. *J Biol Chem*. 1997;272:32360-32369.

12. Vasseur S, Mallo GV, Fiedler F, et al. Cloning and expression of the human p8, a nuclear protein with mitogenic activity. *Eur J Biochem*. 1999;259:670-675.

13. Vasseur S, Hoffmeister A, Garcia-Montero A, et al. Mice with targeted disruption of p8gene show increased sensitivity to lipopolysaccharide and DNA microarray analysis of livers reveals an aberrant gene expression response. *BMC Gastroenterol*. 2003;3:25.

14. Barbosa-Sampaio HC, Liu BO, Drynda R, et al. Nupr1 deletion protects against glucose intolerance by increasing beta cell mass. *Diabetologia*. 2013;56:2477-2486.

15. Nagahara R, Matono T, Sugihara T, et al. Gene expression analysis of the activating factor 3/nuclear protein 1 axis in a non-alcoholic steatohepatitis mouse model. *Yonago Acta Med*. 2019;62:36-46.

16. Santofimia-Castaño P, Lan W, Bintz J, et al. Inactivation of NUPR1 promotes cell death by coupling ER-stress responses with necrosis. *Sci Rep*. 2018;8:16999.

17. Emma MR, Iovanna JL, Bachvarov D, et al. NUPR1, a new target in liver cancer: implication in controlling cell growth, migration, invasion and sorafenib resistance. *Cell Death Dis*. 2016;7:e2269.

18. Päth G, Mehana AE, Pilz IH, et al. NUPR1 preserves insulin secretion of pancreatic β-cells during inflammatory stress by multiple low-dose streptozotocin and high-fat diet. *Am J Physiol Metab*. 2020;319:E338-E344.

19. Kleiner DE, Brunt EM, Van Natta M, et al. Design and validation of a histological scoring system for nonalcoholic fatty liver disease. *Hepatology*. 2005;41:1313-1321.

20. Arora S, Patra SK, Saini R. HDL—a molecule with a multi-faceted role in coronary artery disease. *Clin Chim acta*. 2016;452:66-81.

21. Garcia-Montero A, Vasseur S, Mallo GV, Soubeyran P, Dagorn JC, Iovanna JL. Expression of the stress-induced p8 mRNA is transiently activated after culture medium change. *Eur J Cell Biol*. 2001;80:720–725.

22. Brunt EM, Tiniakos DG. Histopathology of nonalcoholic fatty liver disease. *World J Gastroenterol*. 2010;16:5286.

23. Chavez-Tapia NC, Rosso N, Tiribelli C. Effect of intracellular lipid accumulation in a new model of non-alcoholic fatty liver disease. *BMC Gastroenterol*. 2012;12:20.

24. Müller FA, Sturla SJ. Human in vitro models of nonalcoholic fatty liver disease. *Curr Opin Toxicol*. 2019;16:9-16.

25. Kersten S, Stienstra R. The role and regulation of the peroxisome proliferator activated receptor alpha in human liver. *Biochimie*. 2017;136:75-84.

26. Rutkowski DT, Wu J, Back S-H, et al. UPR pathways combine to prevent hepatic steatosis caused by ER stress-mediated suppression of transcriptional master regulators. *Dev Cell*. 2008;15:829-840.

27. Kramer R, Weber TK, Arceci R, et al. Inhibition of N-linked glycosylation of P-glycoprotein by tunicamycin results in a reduced multidrug resistance phenotype. *Br J Cancer*. 1995;71:670-675.

28. Jo H, Choe SS, Shin KC, et al. Endoplasmic reticulum stress induces hepatic steatosis via increased expression of the hepatic very low-density lipoprotein receptor. *Hepatology*. 2013;57:1366-1377.

29. Lee J-S, Zheng Z, Mendez R, Ha S-W, Xie Y, Zhang K. Pharmacologic ER stress induces non-alcoholic steatohepatitis in an animal model. *Toxicol Lett*. 2012;211:29-38.

30. Chowdhury UR, Samant RS, Fodstad O, Shevde LA. Emerging role of nuclear protein 1 (NUPR1) in cancer biology. *Cancer Metastasis Rev*. 2009;28:225-232.

31. Cano CE, Hamidi T, Sandi MJ, Iovanna JL. Nupr1: the Swiss-knife of cancer. *J Cell Physiol*. 2011;226:1439-1443.

32. Mallo GV, Fiedler F, Calvo EL, et al. Cloning and expression of the Rat p8 cDNA, a new gene activated in pancreas during the acute phase of pancreatitis, pancreatic development, and regeneration, and which promotes cellular growth. *J Biol Chem*. 1997;272(51):32360–32369.

33. Vasseur S, Folch-Puy E, Hlouschek V, et al. p8 improves pancreatic response to acute pancreatitis by enhancing the expression of the anti-inflammatory protein pancreatitis-associated protein I. *J Biol Chem*. 2004;279:7199-7207.

34. Huang C, Lan W, Fraunhoffer N, Meilerman A, Iovanna J, Santofimia-Castaño P. Dissecting the anticancer mechanism of trifluoperazine on pancreatic ductal adenocarcinoma. *Cancers*. 2019;11:1869.

35. Ron D, Walter P. Signal integration in the endoplasmic reticulum unfolded protein response. *Nat Rev Mol Cell Biol*. 2007;8:519–529.

36. Lee A, Chu GC, Iwakoshi NN, Glimcher LH. XBP-1 is required for biogenesis of cellular secretory machinery of exocrine glands. *EMBO J*. 2005;24:4368-4380.

37. Lee A-H, Scapa EF, Cohen DE, Glimcher LH. Regulation of hepatic lipogenesis by the transcription factor XBP1. *Science*. 2008;320:1492-1496.

38. Oyadomari S, Harding HP, Zhang Y, Oyadomari M, Ron D. Dephosphorylation of translation initiation factor 2α enhances glucose tolerance and attenuates hepatosteatosis in mice. *Cell Metab*. 2008;7:520-532.

39. Wang S, Kaufman RJ. The impact of the unfolded protein response on human disease. *J Cell Biol*. 2012;197:857-867.

40. Chen X, Zhang F, Gong QI, et al. Hepatic ATF6 increases fatty acid oxidation to attenuate hepatic steatosis in mice through peroxisome proliferator–activated receptor α. *Diabetes*. 2016;65:1904-1915.

41. Taïeb D, Malicet C, Garcia S, et al. Inactivation of stress protein p8 increases murine carbon tetrachloride hepatotoxicity via preserved CYP2E1 activity. *Hepatology*. 2005;42:176-182.

42. Wang C, Huang Z, Du Y, Cheng Y, Chen S, Guo F. ATF4 regulates lipid metabolism and thermogenesis. *Cell Res*. 2010;20:174-184.

43. Fusakio ME, Willy JA, Wang Y, et al. Transcription factor ATF4 directs basal and stress-induced gene expression in the unfolded protein response and cholesterol metabolism in the liver. *Mol Biol Cell*. 2016;27:1536-1551.

44. Allen-Jennings AE, Hartman MG, Kociba GJ, Hai T. The roles of ATF3 in liver dysfunction and the regulation of phosphoe-nolpyruvate carboxykinase gene expression. *J Biol Chem*. 2002;277:20020-20025.

45. Yamamoto K, Takahara K, Oyadomari S, et al. Induction of liver steatosis and lipid droplet formation in ATF6α-knockout mice burdened with pharmacological endoplasmic reticulum stress. *Mol Biol Cell*. 2010;21:2975-2986.

46. Zhu X, Xiong T, Liu P, et al. Quercetin ameliorates HFD-induced NAFLD by promoting hepatic VLDL assembly and lipophagy via the IRE1a/XBP1s pathway. *Food Chem Toxicol*. 2018;114:52-60.

47. Herrema H, Zhou Y, Zhang D, et al. XBP1s is an anti-lipogenic protein. *J Biol Chem*. 2016;291:17394-17404.

SUPPORTING INFORMATION

Additional Supporting Information may be found online in the Supporting Information section.